



Correcting Mode Proportion Bias in Generalized Bayesian Inference via a Weighted Kernel Stein Discrepancy

Elham Afzali^{*}, Saman Muthukumarana[†] and Liqun Wang[†]

Abstract. Generalized Bayesian Inference (GBI) provides a flexible framework for updating prior distributions using various loss functions instead of the traditional likelihoods, thereby enhancing the model robustness to model misspecification. However, GBI often suffers the problem associated with intractable likelihoods. Kernelized Stein Discrepancy (KSD), as utilized in a recent study, addresses this challenge by relying only on the gradient of the log-likelihood. Despite this innovation, KSD-Bayes suffers from critical pathologies, including insensitivity to well-separated modes in multimodal posteriors. To address this limitation, we propose a weighted KSD method that retains computational efficiency while effectively capturing multimodal structures. Our method improves the GBI framework for handling intractable multimodal posteriors while maintaining key theoretical properties such as posterior consistency and asymptotic normality. Experimental results demonstrate that our method substantially improves mode sensitivity compared to standard KSD-Bayes, while retaining robust performance in unimodal settings and in the presence of outliers.

Keywords: Generalized Bayesian Inference, Kernel Stein Discrepancy, Intractable Likelihood, Multimodal Posterior Distributions.

1 Introduction

Bayesian inference provides a principled statistical framework for updating probabilistic beliefs about model parameters based on observed data through the likelihood function. However, classical Bayesian methods typically assume access to tractable likelihoods and well-specified models—conditions that are often violated in complex, real-world scenarios. In such cases, when likelihoods are intractable or misspecified, Bayesian inference can yield misleading conclusions and unreliable predictions.

To address the shortcoming posed by misspecified likelihoods, the Generalized Bayesian Inference (GBI) framework (Bissiri et al., 2016; Jewson et al., 2018) redefines posterior construction by replacing the likelihood with a data-dependent loss function. These loss-based Bayesian paradigms offer a promising solution by modifying how parameter values are evaluated, rather than altering the statistical model itself. This flexibility is particularly valuable in scenarios where the exact nature of the likelihood misspecification cannot be fully characterized. However, GBI introduces additional challenges when the likelihood is intractable, as traditional MCMC methods depend on explicit

^{*}Department of Statistics, University of Manitoba, afzalie@myumanitoba.ca

[†]Department of Statistics, University of Manitoba, saman.muthukumarana@umanitoba.ca; liqun.wang@umanitoba.ca

likelihood evaluations. Without access to the likelihood, both evaluating the posterior and generating samples from it become computationally challenging and, in many cases, impractical without alternative approximations.

Many practical models exhibit intractable likelihoods, where the likelihood function takes the form $p_\theta(x_i) = \frac{q_\theta(x_i)}{Z_\theta}$, while $q_\theta(x_i)$ is straightforward to compute, the normalizing constant $Z_\theta = \int_{\mathcal{X}} q_\theta(x) dx$ is computationally intractable. Consequently, the Bayesian posterior itself also becomes doubly intractable (Murray et al., 2012):

$$\pi_n(\theta) = \pi_0(\theta) \frac{1}{Z_X} \left(\prod_{i=1}^n \frac{1}{Z_\theta} q_\theta(x_i) \right)$$

where $\pi_0(\theta)$ is the prior distribution and Z_X the marginal likelihood, which is also unknown. This double intractability arises in a wide range of models, making traditional Bayesian inference computationally infeasible. Notable examples of such models include spatial interaction models (Besag, 1974; Diggle, 1990), exponential random graph models for social networks (Park and Haran, 2018), lattice models of spatial data (Moore et al., 2020), and gene expression models (Jiang et al., 2022). These models underscore the need for alternative methods that can bypass the challenges posed by double intractability.

One prominent approach to addressing the challenge of intractable likelihoods in GBI is KSD-Bayes (Matsubara et al., 2022), which utilizes the Kernel Stein Discrepancy (KSD) (Chwialkowski et al., 2016; Liu et al., 2016; Gorham and Mackey, 2017) as a proxy loss function. By relying only on the gradient of the log-likelihood (score function), KSD-Bayes circumvents the need for explicit normalization constants and has demonstrated success across a range of challenging models, including exponential graphical models for high-dimensional network inference and precision parameter estimation in exponential family models (Liu et al., 2019).

Despite these advancements, as discussed by (Matsubara et al., 2022), KSD-Bayes exhibits a fundamental limitation in handling multimodal distributions. When the target posterior contains multiple well-separated modes, KSD-based methods often fail to account for their relative weights, producing biased inferences that favor a uniform mix of modes. This issue, known as mode proportion blindness (Gorham et al., 2019; Wenliang and Kanagawa, 2020; Liu et al., 2023), can also make KSD-Bayes sensitive to kernel choices and prone to convergence issues. Crucially, accurately representing the varying proportions of modes is essential for robust Bayesian inference in multimodal settings, making it essential to address this limitation for more reliable inference. This issue hinders accurate posterior exploration in mixture models (Bénard et al., 2024), gene expression models with multimodal behavior (Jiang et al., 2022), and other real-world problems where capturing mode proportions is critical.

Contributions: In this paper, we propose **MS-KSD-Bayes**, a novel extension of KSD-Bayes that addresses mode proportion blindness in generalized Bayesian inference. Our key contributions are: (i) We introduce a **Weighted Stein Operator** with a density-based weighting function, enhancing sensitivity to mode proportions in multimodal distributions. (ii) We define the **Mode-Sensitive Kernel Stein Discrepancy**

(**MS-KSD**) and integrate it into **Generalized Bayesian Inference**, preserving computational tractability while refining mode detection. **(iii)** We establish **theoretical guarantees**, proving that MS-KSD-Bayes recovers correct mode proportions, maintains posterior consistency, and achieves asymptotic normality. The method performs comparably to KSD-Bayes in unimodal cases and significantly outperforms it in multimodal settings.

To the best of our knowledge, **MS-KSD-Bayes** is the first method to systematically address mode proportion blindness in KSD-based approaches within a generalized Bayesian framework. We validate its effectiveness both theoretically and empirically, demonstrating superior accuracy in multimodal problems while retaining efficiency in standard Bayesian inference tasks.

Outline: Section 2 provides background on Generalized Bayesian Inference and Kernel Stein Discrepancy. Section 3 presents MS-KSD-Bayes, explaining its formulation and how it addresses these issues. Section 4 establishes theoretical guarantees, including posterior consistency and asymptotic normality. Section 5 evaluates the method through experiments on synthetic and real-world datasets. Finally, Section 6 summarizes findings and suggests future research directions. All proofs and detailed derivations of the theoretical results are provided in the Supplementary Material (Afzali et al., 2025). Additionally, the experimental code and datasets are available in our GitHub repository <https://github.com/ElhamAfzali/MSKSD-Bayes>.

2 Background

In this section we briefly review *Kernelized Stein Discrepancy* (KSD), *Generalized Bayesian Inference* (GBI), and the *KSD-Bayes* framework. These foundations will be essential for understanding our proposed Mode-Sensitive KSD-Bayes (MS-KSD-Bayes) approach.

Foundational Assumptions. We assume a locally compact, Hausdorff space $\mathcal{X} \subseteq \mathbb{R}^d$ from which an i.i.d. sample $\{x_i\}_{i=1}^n$ is drawn, yielding the empirical measure $\mathbb{Q}_n = \frac{1}{n} \sum_{i=1}^n \delta_{x_i}$. We let $\Theta \subseteq \mathbb{R}^p$ be a Borel-measurable, open, convex, and bounded parameter space, with each $\theta \in \Theta$ inducing a model distribution \mathbb{P}_θ . Where required, \mathbb{P}_θ admits a density p_θ (strictly positive) so that $\nabla \log p_\theta$ is well-defined, and we impose standard integrability conditions ensuring that Stein-based discrepancies and generalized posteriors are well-defined (e.g. $\int \|\nabla \log p_\theta(x)\| d\mathbb{P}_\theta(x) < \infty$).

2.1 Kernelized Stein Discrepancy (KSD)

Kernelized Stein Discrepancy (KSD) is a divergence measure introduced to assess discrepancies between two probability distributions $\mathbb{P}, \mathbb{Q} \in \mathcal{P}(\mathcal{X})$. KSD is particularly useful when the target distribution \mathbb{P} has an intractable normalizing constant (Chwialkowski et al., 2016; Liu et al., 2016; Gorham and Mackey, 2017) and has been extended to discrete distributions (Yang et al., 2018), conditional distributions (Jitkrittum et al., 2020),

and intractable gradient target distributions (Afzali and Muthukumarana, 2023; Fisher and Oates, 2024; Afzali et al., 2024).

At its core, KSD leverages a Stein operator \mathcal{A}_p associated with a density $p(x)$. The Stein operator takes a multivariate function $g(x) = (g_1(x), \dots, g_d(x))^\top \in \mathbb{R}^d$ and constructs a real-valued function $(\mathcal{A}_p g)(x) : \mathbb{R}^d \rightarrow \mathbb{R}$ as follows:

$$(\mathcal{A}_p g)(x) = \langle \nabla \log p(x), g(x) \rangle + \nabla \cdot g(x)$$

where $\nabla \cdot g(x)$ denotes the divergence of g . This constructed function has the key property (Stein identity) which states that under mild regularity conditions, $\mathbb{E}_{x \sim p}[(\mathcal{A}_p g)(x)] = 0$, for all g in a suitable function class \mathcal{G} . Test functions are chosen from a unit-norm ball in the product reproducing kernel Hilbert space (RKHS) $\mathcal{G}(k)^d$.

The Kernelized Stein Discrepancy (KSD) between \mathbb{P}_θ and \mathbb{Q} distributions is then defined as:

$$\text{KSD}(\mathbb{P}_\theta \| \mathbb{Q}) = \sup_{g \in \mathcal{G}(k)} \left| \mathbb{E}_{X \sim \mathbb{P}_\theta} [(\mathcal{A}_p g)(X)] - \mathbb{E}_{X \sim \mathbb{Q}} [(\mathcal{A}_p g)(X)] \right| \quad (1)$$

By leveraging the Stein identity, this simplifies to:

$$\text{KSD}(\mathbb{P}_\theta \| \mathbb{Q}) = \sup_{g \in \mathcal{G}(k)} \left| \mathbb{E}_{X \sim \mathbb{Q}} [(\mathcal{A}_p g)(X)] \right| \quad (2)$$

In practice, for a given sample $\{x_i\}_{i=1}^n$ from \mathbb{Q} , KSD is estimated empirically. Utilizing the reproducing property of the RKHS, the squared KSD corresponds to the squared RKHS norm of the Stein operator applied to the discrepancy between \mathbb{P}_θ and the empirical measure \mathbb{Q}_n , resulting in the following closed-form expression:

$$\begin{aligned} \text{KSD}^2(\mathbb{P}_\theta \| \mathbb{Q}_n) &= \mathbb{E}_{X, X' \sim \mathbb{Q}} [k_p(X, X')] \\ &\approx \frac{1}{n^2} \sum_{i=1}^n \sum_{j=1}^n k_p(x_i, x_j), \end{aligned} \quad (3)$$

where $k_p(x, x')$ is the Stein kernel, defined in terms of the base kernel k and the score function $s_p(x) = \nabla \log p(x)$ as:

$$\begin{aligned} k_p(x, x') &= \text{trace}(\nabla_x \nabla_{x'}^\top k(x, x')) \\ &\quad + \langle s_p(x), \nabla_{x'} k(x, x') \rangle \\ &\quad + \langle s_p(x'), \nabla_x k(x, x') \rangle \\ &\quad + \langle s_p(x), s_p(x') \rangle k(x, x') \end{aligned}$$

KSD is particularly advantageous as it relies only on the score function $s_p(x)$ of p , making it independent of the intractable normalization constant (Gorham and Mackey, 2017). Convergence guarantees are established when using the inverse multi-quadratic (IMQ) kernel, defined as $k(x, x') = (c + \|x - x'\|^2)^{-\beta}$ with $c > 0$ and $\beta \in (0, 1)$. Additionally, the target density p must be *distantly dissipative*, meaning its negative log-density grows sufficiently fast at infinity to counterbalance the kernel's tail effects (Gorham and Mackey, 2017). This condition ensures lighter tails for p , enabling the establishment of KSD convergence rates.

2.2 Generalized Bayesian Inference with KSD

Traditional Bayesian inference updates a prior beliefs π_0 about model parameters $\theta \in \Theta$ based on observed data via the likelihood function. While this framework is optimal under correct specifications, real-world scenarios often involve model misspecification due to simplifying assumptions or incomplete knowledge of the data-generating process, potentially leading to unreliable inferences.

To address this, alternative Bayesian approaches have been developed to enhance robustness, including robust priors (Berger et al., 1994), power posteriors (Holmes and Walker, 2017), coarsened posteriors (Miller and Dunson, 2019), and scoring rule-based inference (Giummolè et al., 2019). Among these, *Generalized Bayesian Inference* (GBI) (Bissiri et al., 2016) provides a flexible framework by replacing the likelihood with a data-dependent loss function $L_n(\theta)$.

For data $\{x_i\}_{i=1}^n$ drawn from \mathbb{Q} , and a prior distribution $\pi_0(\theta)$ over the parameter space Θ , the GBI posterior is given by:

$$\pi_n^\ell(\theta) \propto \pi_0(\theta) \exp\left(-\alpha n L_n(\theta)\right), \quad (4)$$

where $\alpha > 0$ is a scaling parameter, and n is the sample size. When $\alpha = 1$ and $L_n(\theta)$ is the negative average log-likelihood, i.e., $L_n(\theta) = -\frac{1}{n} \sum_{i=1}^n \log p_\theta(x_i)$, this recovers the standard Bayesian posterior.

Choosing a robust loss $L_n(\theta)$ helps mitigate model misspecification without requiring explicit knowledge of the likelihood’s flaws. The properties and limitations of the selected divergence dictate the theoretical behavior of the resulting generalized posterior (Knoblauch et al., 2019). However, implementing divergence-based losses becomes challenging when the likelihood is intractable, which is common in modern statistical models involving complex stochastic processes or high-dimensional data.

KSD-Bayes. In the case of *intractable likelihoods* within the Generalized Bayesian Inference framework, (Matsubara et al., 2022) proposed KSD-Bayes, which utilizes the KSD as a proxy loss function $L_n(\theta) = \text{KSD}^2(\mathbb{P}_\theta || \mathbb{Q}_n)$. The generalized posterior in KSD-Bayes is defined as:

$$\pi_n^{\text{KSD}}(\theta) \propto \pi_0(\theta) \exp\left(-\alpha n \text{KSD}^2(\mathbb{P}_\theta || \mathbb{Q}_n)\right) \quad (5)$$

KSD-Bayes offers notable advantages by circumventing the need for explicit likelihood evaluations and normalizing constants, relying solely on score functions and kernel computations. This approach enhances robustness to model misspecification and ensures computational efficiency through standard MCMC methods, facilitating scalability to high-dimensional models while preserving theoretical properties like posterior consistency and asymptotic normality.

However, KSD-Bayes suffers from mode proportion blindness, meaning it fails to capture the relative weights of well-separated modes (Gorham et al., 2019; Wenliang and Kanagawa, 2020; Liu et al., 2023). This issue arises because KSD-based, and more

broadly score-based, methods often become insensitive to mode proportions within the target distribution. As demonstrated by (Matsubara et al., 2022) (Section 3.5), the score function $\nabla \log p_\theta(x)$ remains largely unchanged across different mode proportions, causing KSD-Bayes to favor an overly uniform mix of modes, leading to biased inferences. (Bénard et al., 2024) formally proved that in a Gaussian mixture model $p_\theta(x) = w_1 \mathcal{N}(x; \mu, \sigma^2) + (1 - w_1) \mathcal{N}(x; -\mu, \sigma^2)$, as μ increases, the inferred mixture weight converges to $w_1^* \approx 0.5$, regardless of the true w_1 , confirming the mode proportion blindness pathology. This limitation undermines the reliability of KSD-Bayes in multimodal posterior inference, where accurately capturing mode contributions is essential. Addressing this issue is crucial for improving its applicability in real-world problems. In the next section, we introduce **MS-KSD-Bayes**, which corrects this pathology by incorporating a density-based weighting mechanism to restore sensitivity to mode proportions.

3 Methodology

We now present Mode-Sensitive KSD-Bayes (MS-KSD-Bayes), an approach designed to mitigate the blind-spot pathology in standard KSD-based inference. Section 3.1 introduces a weighted Stein operator that modifies the standard operator using a density-based weight to emphasize underrepresented modes, followed by the definition of the mode-sensitive Kernel Stein Discrepancy (MS-KSD). In Section 3.2, we integrate MS-KSD within a Generalized Bayesian Inference framework, leading to the MS-KSD-Bayes posterior. Finally, Section 3.3 applies MS-KSD-Bayes to exponential-family models, discussing closed-form updates under conjugacy and computational strategies for non-conjugate cases.

3.1 Weighted Stein Operator and Mode-Sensitive KSD

A key challenge with the standard Langevin Stein operator is its *insensitivity* to the relative weights of well-separated modes. To address this issue, we introduce a density-dependent weight function into the Stein operator. This modification reweights the contribution of different regions, ensuring that underrepresented modes receive sufficient influence in the discrepancy computation while preserving the overall structure of standard KSD.

Let \mathbb{P} be a probability distribution on \mathbb{R}^d with density $p(x)$ and score function $s_p(x) = \nabla \log p(x)$. We define:

Definition 3.1 (Weighted Stein Operator). For a continuous, positive weight function $\omega_\gamma(x)$, the *weighted Stein operator* \mathcal{A}_p^γ acts on a suitable test function $g : \mathbb{R}^d \rightarrow \mathbb{R}^d$ as

$$(\mathcal{A}_p^\gamma g)(x) = \omega_\gamma(x) (\langle \nabla \log p(x), g(x) \rangle + \nabla \cdot g(x)).$$

A popular practical choice for the weight function is

$$\omega_\gamma(x) = \frac{\gamma}{|\log p(x)| + \epsilon} \tag{6}$$

for some $\gamma > 0$ and small $\epsilon > 0$ to avoid singularities. This function modifies the Stein operator by adjusting the contribution of different regions in the sample space. Specifically, it increases in low-density regions, ensuring that underrepresented modes are not ignored in discrepancy computation. Importantly, since $\omega_\gamma(x)$ depends on the log-likelihood, it remains well-defined even when $p(x)$ is unnormalized. The weighting function appears in ratio form across computations, meaning that any additive constant in $\log p(x)$ cancels out. This property ensures that MS-KSD-Bayes can be applied even when the likelihood is intractable. The term $+\epsilon$ prevents division by zero when $p(x)$ is extremely small, maintaining numerical stability. This weighting strategy counteracts the blind-spot pathology of standard KSD by preserving sensitivity to mode proportions in multimodal settings. Additionally, it ensures smooth behavior across the sample space, making MS-KSD more robust in scenarios where modes are well-separated.

Thus, multiplying the Stein operator by ω_γ ensures that low-density regions remain influential while preventing numerical issues, ultimately enhancing the effectiveness of MS-KSD.

Assumption 3.2 (Regularity Conditions). To ensure \mathcal{A}_p^γ is well-defined and has controlled tail behavior, we assume the existence of constants $0 < m \leq M < \infty$ and $C > 0$ such that for all $x \in \mathbb{R}^d$:

$$m \leq \omega_\gamma(x) \leq M, \quad \text{and} \quad \|\nabla \omega_\gamma(x)\| \leq C.$$

Moreover, let $p(x)$ satisfy the following conditions:

1. $\|x\|^{d-1}p(x) \rightarrow 0$ as $\|x\| \rightarrow \infty$.
2. $\int \|\nabla \log p(x)\| dp(x) < \infty$.
3. $\int [\omega_\gamma(x)]^\beta dp(x) < \infty$ for some $\beta > 1$.
4. $\int \|\nabla \log p(x)\|^{\beta/(\beta-1)} d\mathbb{Q}(x) < \infty$, where \mathbb{Q} is a distribution of interest (e.g., the data-generating distribution).
5. $\sup_{x \in \mathbb{R}^d} \omega_\gamma(x) < \infty$ and $\inf_{x \in \mathbb{R}^d} \omega_\gamma(x) > 0$.

These conditions ensure ω_γ is continuous, differentiable, and bounded away from zero, while also controlling the integrability of $\nabla \log p$. They suffice to apply integration by parts and guarantee the Stein identity below.

Proposition 3.3. *Under Assumption 3.2, for any differentiable function g (with bounded derivatives) in the RKHS $\mathcal{G}(k)$,*

$$\int \mathcal{A}_p^\gamma g dp = 0. \tag{7}$$

A proof using integration by parts is given in Section A.1 of the Supplementary Material (Afzali et al., 2025).

This result implies that the expectation of $\mathcal{A}_p^\gamma g$ under p vanishes under mild regularity conditions, forming the backbone of our Stein-based approach.

Vector-Valued RKHS and Matrix-Valued Kernels. We work in a vector-valued reproducing kernel Hilbert space (v-RKHS) \mathcal{G} , associated with a matrix-valued kernel¹ $K : \mathcal{X} \times \mathcal{X} \rightarrow \mathbb{R}^{d \times d}$. Such kernels uniquely determine a function space $h : \mathcal{X} \rightarrow \mathbb{R}^d$ and serve as a foundation for our Stein-based discrepancies. We denote the norm and inner product on \mathcal{G} by $\|\cdot\|_{\mathcal{G}}$ and $\langle \cdot, \cdot \rangle_{\mathcal{G}}$, respectively.

Assumption 3.4. Let K be a symmetric, positive-definite matrix-valued kernel on \mathcal{X} . For a density $p \in \mathcal{P}$, let \mathcal{A}_p^γ be the weighted Stein operator defined over the v-RKHS \mathcal{G} . We assume:

- For each fixed $x \in \mathcal{X}$, the map $g \mapsto \mathcal{A}_p^\gamma[g](x)$ is a continuous linear functional on \mathcal{G} .
- $\mathbb{E}_{X \sim \mathbb{Q}}[\mathcal{A}_p^\gamma \mathcal{A}_p^\gamma K(X, X')] < \infty$, ensuring the requisite expectations exist.

Under Proposition 3.3 (vanishing of the weighted Stein operator’s integral) and Assumption 3.2 (integrability conditions on p and ω_γ), we can now define a *Mode-Sensitive KSD* that remains sensitive to mode proportions, even for well-separated components.

Definition 3.5 (Mode-Sensitive Kernel Stein Discrepancy). Let \mathbb{P}_θ and \mathbb{Q} be probability distributions, and let g be a test function in the vector-valued reproducing kernel Hilbert space (v-RKHS) \mathcal{G} , associated with the kernel $K : \mathcal{X} \times \mathcal{X} \rightarrow \mathbb{R}^{d \times d}$. The Mode-Sensitive Kernel Stein Discrepancy (MS-KSD) between \mathbb{P}_θ and \mathbb{Q} is defined as:

$$\text{KSD}_\gamma(\mathbb{P}_\theta \parallel \mathbb{Q}) = \sup_{g \in \mathcal{G}(k)} \left| \mathbb{E}_{X \sim \mathbb{P}_\theta}[(\mathcal{A}_p^\gamma g)(X)] - \mathbb{E}_{X \sim \mathbb{Q}}[(\mathcal{A}_p^\gamma g)(X)] \right| \quad (8)$$

where the weighted Stein operator \mathcal{A}_p^γ acts on both arguments of K when forming g .

By Proposition 3.3, the term under \mathbb{P}_θ vanishes, so (8) simplifies to

$$\text{KSD}_\gamma(\mathbb{P}_\theta \parallel \mathbb{Q}) = \sup_{g \in \mathcal{G}(k)} \left| \mathbb{E}_{X \sim \mathbb{Q}}[(\mathcal{A}_p^\gamma g)(X)] \right|. \quad (9)$$

Given a dataset $\{x_i\}_{i=1}^n \sim \mathbb{Q}$, we approximate the expectation in (9) using empirical averages. By leveraging the reproducing property of the vector-valued RKHS, we obtain the empirical estimate:

$$\text{KSD}_\gamma^2(\mathbb{P}_\theta \parallel \mathbb{Q}_n) = \mathbb{E}_{X, X' \sim \mathbb{Q}} [k_p^\gamma(X, X')] \approx \frac{1}{n^2} \sum_{i=1}^n \sum_{j=1}^n k_p^\gamma(x_i, x_j), \quad (10)$$

where X and X' are independent samples from \mathbb{Q} , and $k_p^\gamma(x, x')$ is the weighted Stein kernel defined as:

$$\begin{aligned} k_p^\gamma(x, x') &= \omega_\gamma(x) \omega_\gamma(x') \left[\text{trace}(\nabla_x \nabla_{x'}^\top k(x, x')) \right. \\ &\quad \left. + \langle s_p(x), \nabla_{x'} k(x, x') \rangle \right] \end{aligned}$$

¹For more information about matrix-valued kernels, refer to (Carmeli et al., 2006, 2010)

$$\begin{aligned}
& + \langle s_p(x'), \nabla_x k(x, x') \rangle \\
& + \langle s_p(x), s_p(x') \rangle k(x, x') \Big]. \tag{11}
\end{aligned}$$

This empirical estimate enables practical computation of the MS-KSD by leveraging sample-based approximations of the Stein kernel expectations. Full proofs and derivations of the empirical form are deferred to Section A.2 of the supplementary Material (Afzali et al., 2025).

3.2 MS-KSD-Bayes Posterior

We now incorporate MS-KSD into Generalized Bayesian Inference to construct *MS-KSD-Bayes*. Unlike standard likelihood-based Bayesian inference, KSD-Bayes bypasses the need for intractable normalizing constants by using a Stein-based discrepancy. MS-KSD further refines this by reweighting the Stein operator to ensure robustness in multimodal settings, making it a more expressive alternative to standard KSD-Bayes. The MS-KSD posterior follows the same form as the standard KSD-Bayes posterior, replacing the standard KSD loss with the mode-sensitive loss. This leads to the following definition:

Given a dataset $\{x_i\}_{i=1}^n \sim \mathbb{Q}$ and a prior $\pi_0(\theta)$ over Θ , the MS-KSD-Bayes posterior is defined as:

$$\pi_n^{\text{KSD}_\gamma}(\theta) \propto \pi_0(\theta) \exp\left(-\alpha n \text{KSD}_\gamma^2(\mathbb{P}_\theta \| \mathbb{Q}_n)\right), \tag{12}$$

where $\alpha > 0$ controls the relative influence of the MS-KSD-based loss. This formulation retains the advantages of standard KSD-Bayes while incorporating a mode-sensitive weighting function. Notably, since $\omega_\gamma(x)$ only appears in ratio form, any normalizing constant for ω_γ is absorbed into the overall proportionality constant.

3.3 Generalized Bayesian Inference for Exponential Family Models

We conclude by demonstrating how MS-KSD-Bayes applies to natural exponential families with **conjugate priors**. Let $(\mathcal{X}, \mathcal{F})$ be a measurable space and $\Theta \subseteq \mathbb{R}^p$ be the parameter space. A parametric family of probability distributions $\{P_\theta : \theta \in \Theta\}$ is called an exponential family if its probability density function takes the form:

$$p_\theta(x) = \exp\left(\xi(\theta)^\top t(x) - a(\theta) + b(x)\right) \tag{13}$$

where $t : \mathcal{X} \rightarrow \mathbb{R}^p$ is a sufficient statistic, $a : \Theta \rightarrow \mathbb{R}$ is the log-normalizing function, and $b : \mathcal{X} \rightarrow \mathbb{R}$ is a carrier measure. This formulation encompasses a broad class of statistical models, including those with intractable normalization constants $\exp(a(\theta))$, which are prevalent in modern machine learning applications (Canu and Smola, 2006). Our weighted operator approach *does not require* explicit knowledge of $a(\theta)$, as we only need $\nabla \log p_\theta(x)$, which can be computed or approximated from unnormalized log-density forms. The weighting factor $\omega_\gamma(x)$ similarly only needs $\log p_\theta(x)$ up to additive constants, since it is used in ratio form as $\omega_\gamma(x) = \frac{\gamma}{|\log p(x)| + \epsilon}$.

Proposition 3.6. Consider a natural exponential family \mathbb{P}_θ on \mathbb{R}^d and a prior $\pi_0(\theta)$. The MS-KSD-Bayes posterior takes the form:

$$\pi_n^{KSD\gamma}(\theta) \propto \pi_0(\theta) \times e^{-\alpha n[\theta^T \cdot \Gamma_n \theta + \theta \cdot \tau_n]} \quad (14)$$

where $\Gamma_n \in \mathbb{R}^{p \times p}$ and $\tau_n \in \mathbb{R}^p$. For a natural exponential family ($\xi(\theta) = \theta$), and a Gaussian prior $\pi_0(\theta) \propto \exp(-\frac{1}{2}(\theta - \mu_0) \cdot \Sigma_0^{-1}(\theta - \mu_0))$, the generalised posterior becomes:

$$\pi_n^D(\theta) \propto \exp(-\frac{1}{2}(\theta - \mu_n) \cdot \Sigma_n^{-1}(\theta - \mu_n)) \quad (15)$$

, where

$$\Sigma_n^{-1} := \Sigma_0^{-1} + 2\alpha n \Gamma_n$$

and

$$\mu_n := \Sigma_n(\Sigma_0^{-1}\mu_0 + \alpha n \tau_n)$$

Full derivation and explicit expressions for Γ_n, τ_n appear in Section A.3 of the Supplementary Material (Afzali et al., 2025).

For **non-conjugate** inference scenarios, conventional Markov Chain Monte Carlo (MCMC) algorithms can be employed to draw samples from the generalized posterior distribution. The computational cost per iteration is closely tied to the evaluation of the MS-KSD, which requires summing over all data point pairs. This results in a computational complexity of $O(n^2)$ as standard KSD, due to the double summation inherent in kernel evaluations.

However, components of the MS-KSD formula that are independent of the parameter θ , such as $k(x, x')$, can be precomputed and stored before the iterative process begins. These precomputed values can then be reused during inference, significantly reducing the computational burden per iteration by eliminating redundant calculations.

To further enhance computational efficiency, recent studies have introduced stochastic approximation techniques (Huggins and Mackey, 2018; Gorham et al., 2020). These methods involve utilizing mini-batches of data to compute unbiased estimates of the KSD, reducing the computational complexity from $O(n^2)$ to $O(B^2)$, where $B \ll n$ denotes the mini-batch size.

In summary, MS-KSD-Bayes preserves the intractable-likelihood advantages of KSD-based inference while *improving sensitivity to multimodal structure*, especially when some modes are small but practically important. This capability is particularly useful in high-dimensional mixture modeling, gene expression data, and other applications where accurately tracking all modes is essential.

4 Theoretical Results for MS-KSD-Bayes

This section outlines the principal asymptotic properties of MS-KSD-Bayes, including posterior consistency and a Bernstein–von Mises theorem. All technical proofs are deferred to the appendix, and the assumptions on boundedness, integrability, and smoothness of the weighted Stein operator \mathcal{A}_p^γ (including the weight function ω_γ) follow from Section 3 and Assumptions 3.2–3.4.

Theorem 4.1 (Posterior Consistency for MS-KSD-Bayes). *Let $\Theta \subset \mathbb{R}^p$ be an open, convex parameter space and $\theta_* \in \Theta$ minimize $\text{KSD}_\gamma^2(\mathbb{P}_\theta \| p)$. Consider the MS-KSD-Bayes posterior*

$$\pi_n^{\text{KSD}_\gamma}(\theta) \propto \pi_0(\theta) \exp(-\alpha n \text{KSD}_\gamma^2(\mathbb{P}_\theta \| \mathbb{Q}_n)),$$

where $\alpha > 0$, $\omega_\gamma(x)$ satisfies Assumptions 3.2–3.4, and $\pi_0(\theta)$ is strictly positive in a neighborhood of θ_* . Then, under mild integrability and smoothness conditions:

$$\lim_{n \rightarrow \infty} \pi_n^{\text{KSD}_\gamma}(U) = 1 \quad \text{a.s.}$$

for any open set $U \subset \Theta$ containing θ_* . Specifically:

a) *Pointwise Convergence:* For each fixed $\theta \in \Theta$,

$$\text{KSD}_\gamma^2(\mathbb{P}_\theta \| \mathbb{Q}_n) \xrightarrow{\text{a.s.}} \text{KSD}_\gamma^2(\mathbb{P}_\theta \| p).$$

b) *Uniform Convergence:* Under additional regularity (e.g., bounded derivatives, equicontinuity),

$$\sup_{\theta \in \Theta} |\text{KSD}_\gamma^2(\mathbb{P}_\theta \| \mathbb{Q}_n) - \text{KSD}_\gamma^2(\mathbb{P}_\theta \| p)| \xrightarrow{\text{a.s.}} 0.$$

c) *Strong Consistency:* The posterior concentrates around θ_* ,

$$\pi_n^{\text{KSD}_\gamma}(U) \xrightarrow{\text{a.s.}} 1.$$

Discussion. This consistency result extends that of standard KSD-Bayes by incorporating the bounded, density-driven weight ω_γ . Using V-statistic arguments, we establish almost sure pointwise convergence of KSD_γ^2 . Additional smoothness ensures uniform convergence, leading the posterior to concentrate around θ_* . The strictly positive prior in neighborhoods of θ_* ensures consistency, aligning with generalized Bayesian inference principles. The full proof is provided in Section A.4 of the Supplementart Material (Afzali et al., 2025).

Theorem 4.2 (Bernstein–von Mises for MS-KSD-Bayes). *In addition to the assumptions required for consistency, suppose $\text{KSD}_\gamma^2(\mathbb{P}_\theta \| p)$ is three times continuously differentiable in a neighborhood of θ_* . Let*

$$H_* = \nabla_\theta^2 \text{KSD}_\gamma^2(\mathbb{P}_\theta \| p) \Big|_{\theta=\theta_*},$$

assumed nonsingular. Consider the MS-KSD-Bayes posterior

$$\pi_n^{\text{KSD}_\gamma}(\theta) \propto \pi_0(\theta) \exp\left[-\alpha n \text{KSD}_\gamma^2(\mathbb{P}_\theta \| \mathbb{Q}_n)\right].$$

If $\hat{\theta}_n$ is the posterior mean or mode and \hat{H}_n is a consistent estimator of H_* (for instance, computed from local second derivatives of the weighted KSD), then as $n \rightarrow \infty$, the

posterior distribution converges in total variation to a Gaussian with center $\hat{\theta}_n$ and covariance \hat{H}_n^{-1} . Formally, for any Borel set $A \subseteq \mathbb{R}^p$,

$$\int_A |\pi_n^{\text{KSD}\gamma}(d\theta) - Z_n^{-1} \exp(-\frac{1}{2}(\theta - \hat{\theta}_n)^\top \hat{H}_n(\theta - \hat{\theta}_n))| \xrightarrow{\text{a.s.}} 0$$

where $Z_n = \sqrt{(2\pi)^p \det(\hat{H}_n^{-1})}$.

Discussion. The Bernstein–von Mises (BvM) theorem for MS-KSD-Bayes demonstrates that, under appropriate smoothness conditions, the posterior distribution asymptotically approximates a multivariate normal distribution centered at $\hat{\theta}_n$ with covariance \hat{H}_n^{-1} . The boundedness of $\omega_\gamma(x)$ ensures that the partial derivatives of $\text{KSD}_\gamma^2(\mathbb{P}_\theta \| p)$ are well-controlled, facilitating the local Taylor expansion around θ_* and the application of Laplace approximation techniques. This result parallels classical BvM theorems in Bayesian nonparametrics and generalized Bayesian frameworks (Kleijn and Van der Vaart, 2012; Bissiri et al., 2016), with the bounded weight $\omega_\gamma(x)$ playing a crucial role in maintaining regularity. The full proof is provided in Section A.5 of the Supplementary Material (Afzali et al., 2025).

Remark 4.3 (Convergence Rate Preservation). Under standard regularity conditions, the convergence rate of MS-KSD-Bayes matches that of KSD-Bayes. Specifically, if ω_γ is bounded as $0 < c_1 \leq \omega_\gamma(x) \leq c_2 < \infty$ for some constants c_1, c_2 , then for any consistent sequence of estimators $\hat{\theta}_n$ (such as the posterior mean),

$$|\hat{\theta}_n - \theta_*| = O_p(n^{-1/2})$$

where θ_* is the true parameter. The weighting affects only the constants in the asymptotic expansion, not the fundamental $n^{-1/2}$ rate characteristic of parametric problems.

4.1 Theoretical Considerations and Practical Implications

While MS-KSD-Bayes enhances the robustness of KSD-based inference by incorporating mode sensitivity, its effectiveness depends on the structure of the target distribution and the proper choice of weighting function. In this section, we discuss potential failure cases and practical considerations that may impact its stability and reliability, along with strategies to mitigate these issues.

III-Defined Log-Density and Divergent Weighting. The weighting function $\omega_\gamma(x)$ relies on $\log p(x)$, which must be well-defined across the domain. If $\log p(x)$ exhibits singularities or vanishes too sharply in certain regions, the weighting function can diverge, leading to instability in the MS-KSD computation. This issue commonly arises in distributions with sharp density cutoffs or degenerate support.

To prevent instability, a truncated weighting function can be used:

$$\tilde{\omega}_\gamma(x) = \frac{\gamma}{\max(|\log p(x)|, \tau) + \epsilon} \quad (16)$$

where τ prevents excessive weighting in extreme regions, ensuring numerical stability.

Mode Separation and Weighting Sensitivity. MS-KSD is most effective in distributions with well-separated modes. However, when modes are closely spaced or nearly overlapping, the weighting function may fail to sufficiently distinguish them, reducing the effectiveness of mode-sensitive adjustments. Moreover, improper tuning of γ may result in either over-amplification of tail regions or insufficient emphasis on underrepresented areas.

A practical approach to address this is to use an adaptive weighting mechanism, where γ is adjusted dynamically based on local density estimates rather than being fixed. This allows the method to better adapt to different modal structures within the data.

Heavy-Tailed and Discontinuous Distributions. For heavy-tailed distributions, standard moment conditions required for Stein-based methods may not hold, leading to divergent expectations. Similarly, in cases where $p(x)$ exhibits sharp discontinuities, integration by parts may fail unless additional smoothness conditions are imposed.

To ensure proper Stein calculations, one can enforce a decay constraint on $p(x)$:

$$p(x) \leq Ce^{-\alpha\|x\|} \quad (17)$$

for some constants $C, \alpha > 0$, ensuring finiteness of expectations and valid Stein computations. If such constraints cannot be imposed, an alternative is to regularize the kernel to accommodate discontinuities.

Computational Complexity and Kernel Choice. MS-KSD-Bayes introduces an additional weighting function into the standard KSD framework, which may increase computational complexity, particularly for large datasets. The empirical MS-KSD estimate involves a double sum over n , leading to an $\mathcal{O}(n^2)$ complexity. To improve scalability, low-rank approximations such as Nyström sampling or random Fourier features can be used to reduce the kernel evaluation cost.

5 Experiment Design

Following the approach in the KSD-Bayes benchmark study (Matsubara et al., 2022), we employ the *Kernel Exponential Family* (KEF) model to compare the performance of MS-KSD-Bayes against KSD-Bayes. This framework provides a flexible yet computationally efficient way to model complex distributions, particularly when normalizing constants are intractable. In what follows, we showcase MS-KSD-Bayes’ ability to infer correct mode proportions in two different multimodal settings. Section 5.1 examines the widely studied *Galaxy* dataset, a classic benchmark for comparing multimodal inference methods, while Section 5.2 focuses on a real-world *Lung Cancer Gene Expression* dataset, offering insight into more complex, biologically driven mode structures. These experiments collectively highlight how MS-KSD-Bayes overcomes key limitations of KSD-Bayes by more accurately capturing well-separated modes.

Generalized Bayesian KEF Formulation. In this setting, the probability density function is written as

$$p_{\theta}(x) \propto q(x) \exp\left(\langle f, \kappa(\cdot, x) \rangle_{\mathcal{G}(\kappa)}\right), \quad (18)$$

where $q(x)$ is the reference density, chosen to be $\mathcal{N}(0, S^2)$ with S denoting the width (standard deviation) of the reference measure, $\kappa(x, y)$ is the reproducing kernel (here, a Gaussian RBF kernel), and f lies in the corresponding Reproducing Kernel Hilbert Space (RKHS) $\mathcal{G}(\kappa)$. This approach allows for a nonparametric representation of probability distributions. To avoid computing the typically intractable normalizing constant, we approximate $f(x)$ by a finite-rank expansion $f(x) = \sum_{i=1}^p \theta_{(i)} \phi_{(i)}(x)$, where $\{\phi_{(i)}(x)\}_{i=1}^p$ are suitable basis functions, and $\theta_{(i)}$ are coefficients to be inferred. We adopt Hermite polynomials as basis functions $\phi_{(j+1)}(x) = \frac{x^j}{\sqrt{j!}} \exp(-x^2/2)$ which ensures numerical stability and an effective approximation within the RKHS. The parameter vector $\theta_{(i)}$ follows independent Gaussian priors $\theta_{(i)} \sim \mathcal{N}(0, L^2 i^{-\beta})$, where L is a global scale parameter governing the overall prior variance, and β adjusts how aggressively higher-order terms are shrunk.

We employ the Inverse Multi-Quadratic (IMQ) kernel due to its favorable convergence properties in Stein-based methods. In the experiments described below, we focus on MS-KSD-Bayes' ability to capture correct mode proportions in multimodal settings, thus demonstrating how it mitigates the limitations of KSD-Bayes in scenarios with well-separated modes.

Integration of α and γ . In the baseline KSD-Bayes framework, the generalized posterior is controlled by a single scaling parameter, α . In contrast, MS-KSD-Bayes introduces an additional weighting factor, γ . For direct comparability, we set $\alpha = 1$ in KSD-Bayes (matching the original configuration in (Matsubara et al., 2022)), while in MS-KSD-Bayes we fix $\alpha \cdot \gamma = 1$. This ensures both methods share a comparable overall scale, facilitating stable and consistent performance across all experiments.

5.1 Galaxy Velocity Data Experiments

To evaluate the performance of MS-KSD-Bayes in multimodal settings, we replicate the KSD-Bayes experiment from prior work using the *Galaxy* velocity dataset (Postman et al., 1986; Roeder, 1990), which comprises $n = 82$ velocity measurements (in km/sec) from six distinct conic sections of a survey of the Corona Borealis galaxy cluster. This dataset is well-known for its multimodal structure, making it an ideal benchmark for mode-sensitive inference. For this experiment, we adopt $p = 25$ Hermite polynomial basis functions within the KEF framework, set the reference density to $q(x) = \mathcal{N}(0, 3^2)$ (hence $S = 3$), and use a Gaussian RBF kernel $\kappa(x, y) = \exp(-\frac{(x-y)^2}{2})$. We also fix $L = 10$ as the global prior scale, and set $\beta = 1.1$ ensuring consistency with the original KSD-Bayes configuration. These choices collectively enable us to focus on how MS-KSD-Bayes compares to KSD-Bayes in capturing distinct modes and accurately reflecting their relative proportions.

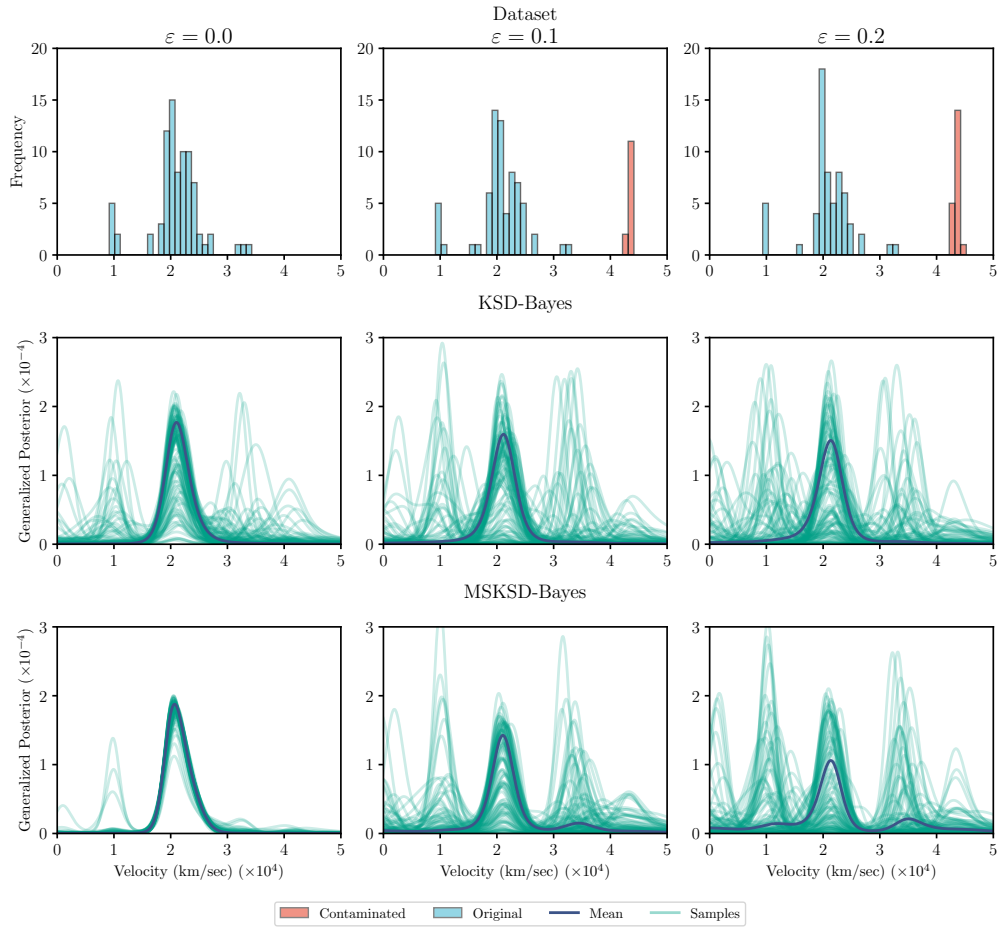


Figure 1: Posterior density estimation for the galaxy dataset. The first row shows the data histogram. The second row presents KSD-Bayes estimates, which fail to capture mode proportions. The third row shows MS-KSD-Bayes estimates, accurately reflecting the multimodal structure.

Sensitivity to Mode Proportions. A major drawback of KSD-Bayes is its insensitivity to mode proportions when modes are well-separated. This issue results in an equal weighting of modes, even when the true proportions differ. To introduce a controlled secondary mode, we contaminate the Galaxy velocity data by replacing a fraction ϵ of the observations with samples drawn from $\mathcal{N}(y, 0.1^2)$ with $y = 5$. This setup allows us to assess whether the benchmark models can accurately capture bimodality or if they remain biased toward a unimodal posterior.

Figure 1 compares the generalized posterior densities generated by KSD-Bayes and MS-KSD-Bayes across three contamination levels ($\epsilon = 0.0, 0.1, \text{ and } 0.2$). In the top row,

histograms of the data reveal that the original Galaxy dataset ($\epsilon = 0$) features multiple peaks that are not sharply separated. As ϵ increases, a clear secondary peak develops near velocity $\approx 5 \times 10^4$, providing a direct test of each method’s capacity to capture multiple modes. When $\epsilon = 0$, both KSD-Bayes and MS-KSD-Bayes return unimodal posterior estimates, indicating that neither method falsely detects multiple modes when they are not distinctly separated.

As soon as the contamination level increases to $\epsilon = 0.1$, the well-separated secondary mode near $\approx 5 \times 10^4$ becomes distinctly visible (see Figure 1). MS-KSD-Bayes successfully distinguishes this additional peak from the primary mode, accurately capturing the bimodal nature of the data. In contrast, KSD-Bayes remains insensitive to the change, continuing to estimate a unimodal posterior. At the higher contamination level of $\epsilon = 0.2$, this contrast persists: MS-KSD-Bayes continues to detect both peaks and preserve their relative proportions, whereas KSD-Bayes still fails to identify the second mode. These findings underscore MS-KSD-Bayes’s heightened sensitivity to well-separated modes, and its ability to provide a more faithful representation of the underlying multimodal structure.

5.2 Lung Cancer Gene Expression Experiments

Motivation for Gene Expression Analysis. Accurately capturing multiple modes in gene expression data is crucial, as distinct tumor subtypes often display divergent expression patterns. In this experiment, we examine whether MS-KSD-Bayes can effectively detect and appropriately weight multiple modes in a genomic context by focusing on a well-separated bimodal gene.

In this experiment We evaluate both MS-KSD-Bayes and KSD-Bayes on a lung cancer gene expression dataset from the `oompaData` library for R (Coombes, 2024; R Core Team, 2024; Abrams et al., 2018; Asiaee et al., 2020). This dataset (`lung.dataset`) comprises log-transformed expression values for 150 genes measured in 444 tumor samples, along with clinical annotations contained in `lung.clinical`. The expression data were processed using the transformation $\log_2(1 + x)$, and a subset of genes was selected for illustrative purposes; complete details are available under GEO accession GSE68571.

To identify a probe set with a bimodal profile, we applied the `bimodalIndex` function from the `BimodalIndex` package (Coombes, 2019; Wang et al., 2009) to each gene in `lung.dataset`. This function fits a two-component Gaussian mixture model and computes a *Bimodality Index* (BI) that quantifies both the separation of the modes and their relative proportions (Wang et al., 2009). Ranking the BI values, we identified AFFX-R2-EC-BIOD-5_AT—an Affymetrix probe set identifier—as the most strongly bimodal (BI = 3.49).

For this probe set, we compared MS-KSD-Bayes and KSD-Bayes using the same KEF-based approach as in Section 5.1. In our analysis, we set $p = 10$ for the number of Hermite polynomial basis functions, selected a reference density $q(x) = \mathcal{N}(0, 4^2)$ (i.e., $S = 4$), and fixed the global prior scale at $L = 9$ with an exponent $\beta = 1.2$. All other experimental details, including the use of a Gaussian RBF kernel and the generalized Bayesian framework, mirror those employed in the Galaxy data experiments.

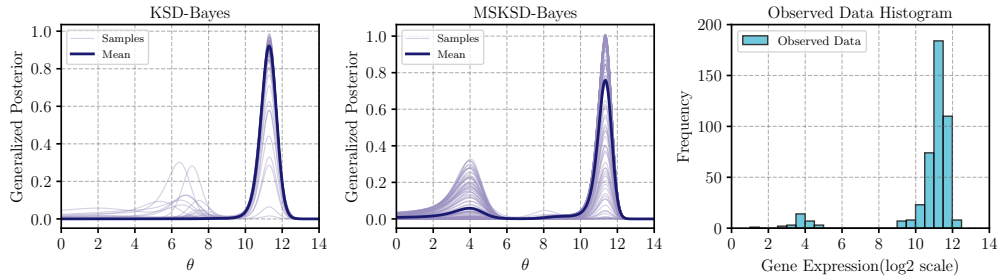


Figure 2: Genralized Posterior Density Estimates for Lung Cancer Gene Expression Data (Setting: $p = 10$, $L = 4$, prior scale=81, prior decay=1.2). Row 1: Histogram of gene expression data. Row 2: KSD-Bayes posterior estimate. Row 3: MS-KSD-Bayes posterior estimate. MS-KSD-Bayes captures the bimodal structure, unlike KSD-Bayes.

Figure 2 presents the results of the generalized posterior distribution estimation for the lung cancer gene expression dataset using both KSD-Bayes and MS-KSD-Bayes. The left panel displays a histogram of the gene expression data, suggesting an underlying multimodal distribution. The middle panel shows the generalized posterior density estimate obtained via standard KSD-Bayes, which yields a unimodal posterior and fails to capture the potential multimodal nature of the data. In contrast, the right panel presents the posterior density estimate derived from MS-KSD-Bayes, which successfully identifies and captures two distinct modes, providing a posterior density estimate that more accurately reflects the data’s distributional characteristics. This visual comparison underscores the mode sensitivity of MS-KSD-Bayes.

The density-based weighting mechanism in MS-KSD-Bayes enhances mode sensitivity, yielding posterior inferences that better capture the potentially multimodal nature of the gene expression data. By preserving the underlying distribution and demonstrating robustness in handling well-separated modes, MS-KSD-Bayes effectively identifies distinct biological subpopulations. Additionally, its density-dependent weighting function mitigates mode proportion bias, yielding more reliable posterior estimates. These properties make MS-KSD-Bayes a powerful and robust alternative for Bayesian inference in complex biomedical applications.

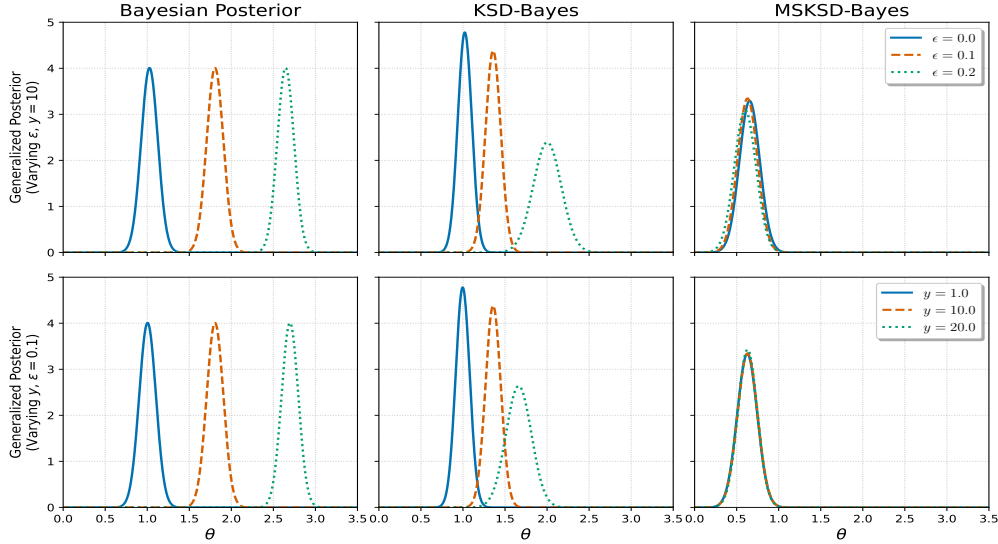


Figure 3: Generalized Posterior distributions for a Gaussian location model under various contamination proportions (ϵ , top row) and outlier displacements (y , bottom row). The three columns compare (left) standard Bayesian inference with a conjugate prior, (center) the KSD-Bayes method, and (right) the proposed MS-KSD-Bayes approach. While the first two methods shift noticeably away from the true mean $\theta_\star = 1$ as ϵ or y increases, MS-KSD-Bayes remains tightly concentrated near θ_\star throughout.

5.3 Gaussian Location Experiment: Unimodal Setting with Contamination

Having demonstrated in Sections 5.1 and 5.2 that MS-KSD-Bayes effectively resolves the mode-proportion blindness issue for distributions with well-separated modes, we now examine its performance in a unimodal Gaussian location setup subject to outlier contamination. This experiment follows the identical design introduced in (Matsubara et al., 2022) for KSD-Bayes, thus enabling a direct comparison. Specifically, we simulate data $X_i \in \mathbb{R}$ from $P_\theta = \mathcal{N}(\theta_\star, 1)$ with $\theta_\star = 1$. To showcase the robustness of the proposed method, MS-KSD-Bayes, we generate these observations from a contaminated process: with probability $1 - \epsilon$, each x_i is drawn from the true distribution $\mathcal{N}(1, 1)$, or else shifted to a large displacement drawn from $\mathcal{N}(y, 1)$. The sample size is fixed at $n = 100$, and the parameter θ receives a $\mathcal{N}(0, 1)$ prior. The resulting dataset is unimodal in the main cluster at $x = 1$ but contains an increasing fraction of outliers for higher ϵ or y .

Figure 3 presents the posterior distributions under three procedures: (i) standard Bayesian updating with a conjugate normal prior, (ii) the non-weighted KSD-Bayes estimator, and (iii) the proposed MS-KSD-Bayes method. Although the standard Bayesian posterior exhibits substantial shifts away from $\theta_\star = 1$ as the contamination level or displacement grows, and the KSD-Bayes posterior demonstrates only partial resistance

to outliers, the MS-KSD-Bayes posterior remains closely centered on the true parameter even for more extreme contamination. Furthermore, no discernible broadening in MS-KSD-Bayes occurs, indicating that the weighting mechanism effectively curbs the impact of far-reaching data points without sacrificing posterior sharpness.

These results underscore that MS-KSD-Bayes not only addresses multimodal complexities but also offers superior robustness in a unimodal regime when faced with contamination. By attenuating the influence of low-density observations, the weighted Stein-based loss ensures that extreme outliers do not unduly bias or inflate the posterior, surpassing both standard Bayesian inference and non-weighted KSD-Bayes in maintaining accurate and stable estimates.

6 Conclusion and Future Work

We have introduced *MS-KSD-Bayes*, a novel approach that overcomes the mode proportion blindness commonly observed in KSD-based methods for generalized Bayesian inference when dealing with intractable likelihoods. The central innovation lies in incorporating a density-weighted Stein operator, which augments the standard Kernel Stein Discrepancy with a density-dependent weighting function. This modification not only highlights underrepresented modes in multimodal distributions but also preserves key theoretical guarantees, including posterior consistency and asymptotic normality, under standard regularity conditions.

Empirical studies on both synthetic data (e.g., Galaxy velocity measurements) and real-world datasets (e.g., lung cancer gene expression) confirm that MS-KSD-Bayes more accurately captures multiple well-separated modes and their relative proportions compared to conventional KSD-Bayes, which tends to favor an overly uniform mix of modes. Moreover, our experiments in a unimodal Gaussian location setting subject to outlier contamination show that MS-KSD-Bayes remains tightly concentrated around the true parameter despite significant contamination, surpassing both standard Bayesian inference and KSD-Bayes in terms of robustness. Hence, the proposed framework closes a critical gap in generalized Bayesian inference by offering robust and computationally feasible posterior exploration in scenarios where existing likelihood-based methods are impeded by intractable normalizing constants or model misspecifications, or unexpected contamination.

Several promising directions remain for future work. First, extending MS-KSD-Bayes to discrete settings, including graph structures and spatial models, holds substantial potential for broadening its applicability. Second, adaptive or hierarchical schemes for learning the weight function ω_γ may further improve the method’s flexibility and stability. Third, incorporating stochastic approximation or mini-batching techniques could alleviate the intrinsic $O(n^2)$ complexity of kernel evaluations, thus enabling efficient inference on large-scale datasets. Additionally, while the inverse multi-quadratic (IMQ) kernel is commonly employed in Stein-based methods, systematically examining other kernel choices tailored to the weighted Stein operator could yield further performance gains.

Further theoretical developments, such as analyzing near-degenerate modes and deriving finite-sample convergence rates, would deepen our understanding of both the method’s strengths and its limitations. Moreover, deploying MS-KSD-Bayes to diverse applications—ranging from multi-population genomic studies to financial risk modeling or time-series analysis—can provide valuable insights into how its enhanced mode sensitivity translates into improved inferential performance. By addressing these research opportunities, MS-KSD-Bayes can be established as a versatile and powerful tool for robust Bayesian inference in increasingly complex and high-dimensional domains.

Funding

The research is partially supported by grants from the Natural Sciences and Engineering Research Council of Canada (NSERC).

Supplementary Material

Supplementary Material for "Correcting Mode Proportion Bias in Generalized Bayesian Inference via a Weighted Kernel Stein Discrepancy" (Afzali et al., 2025). This supplementary document provides detailed proofs of all theorems and propositions presented in the main manuscript, along with full derivations and supporting calculations.

References

- Abrams, Z. B., Zucker, M., Wang, M., Asiaee Taheri, A., Abruzzo, L. V., and Coombes, K. R. (2018). “Thirty biologically interpretable clusters of transcription factors distinguish cancer type.” *BMC genomics*, 19: 1–14. 16
- Afzali, E. and Muthukumarana, S. (2023). “Gradient-free kernel conditional stein discrepancy goodness of fit testing.” *Machine Learning with Applications*, 12: 100463. 4
- Afzali, E., Muthukumarana, S., and Wang, L. (2024). “Navigating interpretability and alpha control in GF-KCSD testing with measurement error: A Kernel approach.” *Machine Learning with Applications*, 17: 100581. 4
- (2025). “Supplementary material for "Correcting Mode Proportion Bias in Generalized Bayesian Inference via a Weighted Kernel Stein Discrepancy"." 3, 7, 9, 10, 11, 12, 20
- Asiaee, A., Abrams, Z. B., Nakayiza, S., Sampath, D., and Coombes, K. R. (2020). “Explaining gene expression using twenty-one micrnas.” *Journal of Computational Biology*, 27(7): 1157–1170. 16
- Bénard, C., Staber, B., and Da Veiga, S. (2024). “Kernel Stein Discrepancy thinning: a theoretical perspective of pathologies and a practical fix with regularization.” *Advances in Neural Information Processing Systems*, 36. 2, 6
- Berger, J. O., Moreno, E., Pericchi, L. R., Bayarri, M. J., Bernardo, J. M., Cano, J. A.,

- De la Horra, J., Martín, J., Ríos-Insúa, D., Betrò, B., et al. (1994). “An overview of robust Bayesian analysis.” *Test*, 3(1): 5–124. 5
- Besag, J. (1974). “Spatial interaction and the statistical analysis of lattice systems.” *Journal of the Royal Statistical Society: Series B (Methodological)*, 36(2): 192–225. 2
- Bissiri, P. G., Holmes, C. C., and Walker, S. G. (2016). “A general framework for updating belief distributions.” *Journal of the Royal Statistical Society: Series B (Statistical Methodology)*, 78(5): 1103–1130. 1, 5, 12
- Canu, S. and Smola, A. (2006). “Kernel methods and the exponential family.” *Neurocomputing*, 69(7-9): 714–720. 9
- Carmeli, C., De Vito, E., and Toigo, A. (2006). “Vector valued reproducing kernel Hilbert spaces of integrable functions and Mercer theorem.” *Analysis and Applications*, 4(04): 377–408. 8
- Carmeli, C., De Vito, E., Toigo, A., and Umanitá, V. (2010). “Vector valued reproducing kernel Hilbert spaces and universality.” *Analysis and Applications*, 8(01): 19–61. 8
- Chwialkowski, K., Strathmann, H., and Gretton, A. (2016). “A kernel test of goodness of fit.” In *International conference on machine learning*, 2606–2615. PMLR. 2, 3
- Coombes, K. R. (2019). *BimodalIndex: The Bimodality Index*. R package version 1.1.9. URL <https://CRAN.R-project.org/package=BimodalIndex> 16
- (2024). *oompaData: Data to Illustrate OOMPA Algorithms*. R package version 3.1.4. URL <https://CRAN.R-project.org/package=oompaData> 16
- Diggle, P. J. (1990). “A point process modelling approach to raised incidence of a rare phenomenon in the vicinity of a prespecified point.” *Journal of the Royal Statistical Society: Series A (Statistics in Society)*, 153(3): 349–362. 2
- Fisher, M. and Oates, C. J. (2024). “Gradient-free kernel Stein discrepancy.” *Advances in Neural Information Processing Systems*, 36. 4
- Giummolè, F., Mameli, V., Ruli, E., and Ventura, L. (2019). “Objective Bayesian inference with proper scoring rules.” *Test*, 28(3): 728–755. 5
- Gorham, J., Duncan, A. B., Vollmer, S. J., and Mackey, L. (2019). “Measuring sample quality with diffusions.” *The Annals of Applied Probability*, 29(5): 2884–2928. 2, 5
- Gorham, J. and Mackey, L. (2017). “Measuring sample quality with kernels.” In *International Conference on Machine Learning*, 1292–1301. PMLR. 2, 3, 4
- Gorham, J., Raj, A., and Mackey, L. (2020). “Stochastic stein discrepancies.” *Advances in Neural Information Processing Systems*, 33: 17931–17942. 10
- Holmes, C. C. and Walker, S. G. (2017). “Assigning a value to a power likelihood in a general Bayesian model.” *Biometrika*, 104(2): 497–503. 5
- Huggins, J. and Mackey, L. (2018). “Random feature Stein discrepancies.” *Advances in neural information processing systems*, 31. 10

- Jewson, J., Smith, J. Q., and Holmes, C. (2018). “Principles of Bayesian inference using general divergence criteria.” *Entropy*, 20(6): 442. 1
- Jiang, X., Xiao, G., and Li, Q. (2022). “A Bayesian modified Ising model for identifying spatially variable genes from spatial transcriptomics data.” *Statistics in medicine*, 41(23): 4647–4665. 2
- Jitkrittum, W., Kanagawa, H., and Schölkopf, B. (2020). “Testing goodness of fit of conditional density models with kernels.” In *Conference on Uncertainty in Artificial Intelligence*, 221–230. PMLR. 3
- Kleijn, B. J. and Van der Vaart, A. W. (2012). “The Bernstein-von-Mises theorem under misspecification.” 12
- Knoblauch, J., Jewson, J., and Damoulas, T. (2019). “Generalized variational inference: Three arguments for deriving new posteriors.” *arXiv preprint arXiv:1904.02063*. 5
- Liu, Q., Lee, J., and Jordan, M. (2016). “A kernelized Stein discrepancy for goodness-of-fit tests.” In *International conference on machine learning*, 276–284. PMLR. 2, 3
- Liu, S., Kanamori, T., Jitkrittum, W., and Chen, Y. (2019). “Fisher efficient inference of intractable models.” *Advances in Neural Information Processing Systems*, 32. 2
- Liu, X., Duncan, A. B., and Gandy, A. (2023). “Using perturbation to improve goodness-of-fit tests based on kernelized stein discrepancy.” In *International Conference on Machine Learning*, 21527–21547. PMLR. 2, 5
- Matsubara, T., Knoblauch, J., Briol, F.-X., and Oates, C. J. (2022). “Robust generalised Bayesian inference for intractable likelihoods.” *Journal of the Royal Statistical Society Series B: Statistical Methodology*, 84(3): 997–1022. 2, 5, 6, 13, 14, 18
- Miller, J. W. and Dunson, D. B. (2019). “Robust Bayesian inference via coarsening.” *Journal of the American Statistical Association*. 5
- Moores, M., Nicholls, G., Pettitt, A., and Mengersen, K. (2020). “Scalable Bayesian inference for the inverse temperature of a hidden Potts model.” 2
- Murray, I., Ghahramani, Z., and MacKay, D. (2012). “MCMC for doubly-intractable distributions.” *arXiv preprint arXiv:1206.6848*. 2
- Park, J. and Haran, M. (2018). “Bayesian inference in the presence of intractable normalizing functions.” *Journal of the American Statistical Association*, 113(523): 1372–1390. 2
- Postman, M., Huchra, J. P., and Geller, M. J. (1986). “Probes of large-scale structure in the Corona Borealis region.” *Astronomical Journal (ISSN 0004-6256)*, vol. 92, Dec. 1986, p. 1238-1247., 92: 1238–1247. 14
- R Core Team (2024). *R: A Language and Environment for Statistical Computing*. R Foundation for Statistical Computing, Vienna, Austria.
URL <https://www.R-project.org/> 16

- Roeder, K. (1990). “Density estimation with confidence sets exemplified by superclusters and voids in the galaxies.” *Journal of the American Statistical Association*, 85(411): 617–624. [14](#)
- Wang, J., Wen, S., Symmans, W. F., Pusztai, L., and Coombes, K. R. (2009). “The bimodality index: a criterion for discovering and ranking bimodal signatures from cancer gene expression profiling data.” *Cancer informatics*, 7: CIN-S2846. [16](#)
- Wenliang, L. K. and Kanagawa, H. (2020). “Blindness of score-based methods to isolated components and mixing proportions.” *arXiv preprint arXiv:2008.10087*. [2](#), [5](#)
- Yang, J., Liu, Q., Rao, V., and Neville, J. (2018). “Goodness-of-fit testing for discrete distributions via Stein discrepancy.” In *International Conference on Machine Learning*, 5561–5570. PMLR. [3](#)